NMR Characterization and Rietveld Refinement of the Structure of Rehydrated AlPO 4 −34

ARTICLE *in* THE JOURNAL OF PHYSICAL CHEMISTRY B · JUNE 2000

Impact Factor: 3.3 · DOI: 10.1021/jp000455a

NMR Characterization and Rietveld Refinement of the Structure of Rehydrated $AlPO_4$-34

Alain Tuel,*,† Stefano Caldarelli,† Anton Meden,‡ Lynne B. McCusker,§ Christian Baerlocher,§ Alenka Ristic,|| Nevenka Rajic,|| Gregor Mali,|| and Venceslav Kaucic||

Institut de Recherches sur la Catalyse, CNRS, Villeurbanne France, University of Ljubljana, Faculty of Chemistry and Chemical Technology, Ljubljana, Slovenia, Laboratory of Crystallography, ETH, Zurich, Switzerland, and National Institute of Chemistry, Ljubljana, Slovenia

Received: February 4, 2000

The triclinic form of $AlPO_4$-34, a microporous aluminophosphate with the chabazite (**CHA**) topology, adopts a rhombohedral symmetry upon calcination. The framework structure of this phase remains intact under ambient conditions, but it distorts dramatically, though reversibly, in the presence of water. Following these structural changes in situ by X-ray diffraction revealed that there are actually two stable rehydrated phases, which differ from each other by one water molecule in the channel. Both of these phases have triclinic unit cells that are closely related to that of the calcined rhombohedral phase. The structure of the low-temperature (10 °C), fully rehydrated phase (phase B) was elucidated by combining high-resolution synchrotron powder diffraction with solid-state NMR techniques. Coordination of three of the six Al atoms to water molecules causes the deformation of the framework and the reduction of the symmetry. Rietveld refinement of the structure of phase B in the triclinic space group $P1$ ($a = 9.026$, $b = 9.338$, $c = 9.508$ Å, $\alpha = 95.1°$, $\beta = 104.1°$, and $\gamma = 96.6°$) converged with $R_F = 0.079$ and $R_{WP} = 0.176$ ($R_{exp} = 0.087$). Framework connectivities derived from the structure were used to assign ^{31}P NMR lines as well as part of the ^{27}Al NMR signal.

Introduction

The synthesis of novel crystalline aluminophosphate molecular sieves ($AlPO_4$-*n*)[1] has been a matter of increasing interest over the two past decades. In contrast to aluminosilicate zeolites, the aluminum species in $AlPO_4$-*n* materials can be four, five, or six-coordinate,[2−4] and this explains why such a large number of structures have been reported. Interest in the field has also been stimulated by the possibility of incorporating tetravalent or divalent cations into the frameworks of these materials and thereby forming potentially active catalysts (MeAPO's) for acidic or redox reactions.[5−8]

Originally, microporous aluminophosphates were prepared in basic media with organic molecules, such as primary amines, as structure-directing agents. The introduction of fluoride ions in the preparation of aluminophosphates allowed novel structures, which could not generally be obtained using the standard route, to be synthesized.[9,10] This strategy was used to make the triclinic form of $AlPO_4$-34, an aluminophosphate with the chabazite (**CHA**) topology.[9−12] Indeed, attempts to synthesize pure $AlPO_4$-34 in the absence of fluoride ions, using conditions that led to the crystallization of MeAPO-34 or SAPO-34, were not successful. However, a synthesis without fluoride using nonconventional phosphorus sources such as $Al(H_2PO_4)_3$ or $H_{10}P_8O_{25}$[13,14] and tetraethylammonium hydroxide as the templating species has been reported. Fluoride ions not only decrease the nucleation rate of aluminophosphates by complexing aluminum but also can play a role as costructuring agents or even be covalently bonded to the framework. In triclinic $AlPO_4$-34, two fluoride ions bridge between two Al atoms in 4-rings connecting double-6-rings of the structure. These two F^- ions neutralize the protonated organic molecule located in the chabazite cage.[11,12]

Upon calcination, both the organic and fluoride species are expelled from the pores, and the template-free material adopts the rhombohedral symmetry of the **CHA** topology. However, the diffraction pattern of this material changes rapidly in the presence of air.[9] Structure modifications of calcined aluminophosphate molecular sieves in the presence of water molecules have been widely reported in the literature.[15−20] They result from the ability of framework aluminum species to modify their coordination in the presence of water. The structure changes are generally reversible, and the original material can be restored by evacuation at relatively low temperature. Structural studies of rehydrated $AlPO_4$-*n* materials are scarce. One of the reasons is that the peaks in the X-ray diffraction patterns of such rehydrated compounds tend to be broad, so structure analysis using Rietveld refinement techniques is difficult.[16,17] Nevertheless, Mentzen et al.[21] were able to refine the structure of rehydrated $AlPO_4$-11 to determine the position of extraframework water molecules inside the channels.

In the present paper, two complementary techniques, X-ray powder profile refinement and solid-state NMR, were applied to elucidate the structure of one of the rehydrated forms of $AlPO_4$-34.

Experimental Section

Synthesis. The reactants used were piperidine (99%, Aldrich), 85% phosphoric acid (Fluka), 40% hydrofluoric acid (Fluka), and aluminum isopropoxide (Aldrich). The relative molar composition of the reaction mixture used in the preparation of $AlPO_4$-34 was Al_2O_3: P_2O_5: HF: 2 piperidine: 100 H_2O. The mixture was prepared by successive addition of phosphoric acid,

* Corresponding author. E-mail: tuel@catalyse.univ-lyon1.fr. Fax: (+33) 4 72 44 53 99.
† Institute de Recherches sur la Catalyse.
‡ University of Ljubljana.
§ Laboratory of Crystallography.
|| National Institute of Chemistry.

10.1021/jp000455a CCC: $19.00
Published on Web 05/26/2000

hydrofluoric acid, and piperidine to a suspension of aluminum isopropoxide in water with constant stirring.

The crystallization was performed at 190 °C for 4 days under static conditions in a Teflon-lined stainless steel autoclave. The products were recovered, washed with distilled water, and dried.

Thermogravimetric Analysis (TGA). Thermogravimetric analysis (TGA) of the calcined hydrated material was performed using a Mettler TA3000 system in the range from 20 to 200 °C with a heating rate of 0.2 °C/min.

Solid-State NMR. All solid-state NMR experiments were performed on a Bruker DSX 400 spectrometer operating at 104.25 and 161.2 MHz for ^{27}Al and ^{31}P nuclei, respectively. Conventional MAS NMR spectra were recorded using a double-bearing probe head equipped with 4-mm (o.d.) zirconia rotors. Samples were spun at the magic angle with a spinning speed of 14 kHz. The pulse lengths were 2 μs (π/4) and 0.7 μs (π/6), and the recycle delays were 30 and 1 s for ^{31}P and ^{27}Al nuclei, respectively.

Two-dimensional 5-quanta (2D-5Q) MAS NMR spectra were collected with a standard 4-mm probe head at a spinning speed of 11 kHz and an RF field of 175 kHz, using a modified RIACT sequence.[22,23] In a typical experiment, 360 scans were accumulated for each free induction decay with a recycle delay of 300 ms. 320 time-domain real data points were acquired in the indirect dimension and pure-phase spectra were obtained by using the TPPI scheme.[24,25] Shearing transformation was applied to the spectra in order to obtain isotropic projections parallel to the f1 direction.[26]

^{27}Al → ^{31}P CP/MAS experiments were performed using a three-channel ^{1}H-X-Y probe head (Bruker) and a conventional spin-lock sequence.[27] Two-dimensional ^{27}Al → ^{31}P CP/MAS correlation experiments were performed by encoding the aluminum evolution frequencies in an initial time period after the 90° pulse. Pure absorption-phase NMR line shapes in both dimensions were obtained by cycling the phase of the 90° pulse using the TPPI scheme. The Hartmann−Hahn matching condition,[28] modified to take only the central ^{27}Al transition into account, was set up experimentally on the rehydrated $AlPO_4$-34 sample. On a static sample, this condition corresponds to:

$$\gamma_P B_{1,P} = 3\gamma_{Al} B_{1,Al}$$

For fast spinning conditions, the matching condition is split up into sidebands shifted by once or twice the spinning frequency:[29]

$$\gamma_P B_{1,P} = 3\gamma_{Al} B_{1,Al} \pm n\nu_R \qquad n = 1 \text{ or } 2$$

Cross-polarization involving quadrupolar nuclei can be difficult because of the sensitive tune-up required for effective spin-locking of the magnetization. This has been shown to work most effectively for low power and high-spinning speeds.[29,30] A spin-locking field of 4 and 5 kHz for ^{27}Al and ^{31}P, respectively, which corresponds to matching with $n = 1$ (spinning rate approximately 7 kHz), was used. Under these conditions, the power level of the irradiation field becomes effective for on-resonance polarization transfer, but it is too weak to overcome the dampening effects of the offset completely. A more homogeneous transfer was achieved by linear amplitude modulation of the spin-locking field on the aluminum.[31]

The contact time was 1.5 ms, which corresponds to the maximum intensity for all ^{31}P NMR signals, and the recycle delay was 0.3 s. Typically, 1024 scans were accumulated for each of the 128 time-domain data points acquired in the aluminum dimension.

TABLE 1: Experimental and Crystallographic Data for Rehydrated $AlPO_4$-34 (Phase B)

data collection	
synchrotron facility	ESRF
beamline	BM1 (Swiss−Norwegian)
wavelength (Å)	0.64791
2θ range (°2θ)	3.70−35.50
step size(°2θ)	0.005
unit cell	
space group	P1
a (Å)	9.026(3)
b (Å)	9.338(2)
c (Å)	9.508(2)
α (°)	95.1(2)
β (°)	104.1(2)
γ (°)	96.6(2)
refinement	
standard peak (hkl, 2θ)	1 0 0, 4.29
peak range (no. of FWHM)	22
no. of observations	6116
no. of contributing reflections	1303
no. of geometric restraints	175
no. of structural parameters	147
no. of profile parameters	11
R_{exp}	0.087
R_{wp}	0.176
χ^2	2.02
R_F	0.079

X-ray Powder Diffraction. Phase transitions during hydration were followed in situ on a Siemens D-5000 diffractometer equipped with a HTK-16 high-temperature chamber, using Cu$K\alpha_1$ radiation. The as-synthesized material was heated in air at 5 °C/min to 700 °C, held at this temperature for 2 h, and then cooled at the same rate to 100 °C. After this procedure, a characteristic part of the diffraction pattern was scanned at 100, 60 and 50 °C and then at constant temperatures in steps of 3 °C down to 17 °C. The sample was then heated to 100 °C and cooled again using the same protocol for data collections.

High-resolution synchrotron powder diffraction data were collected on the Swiss−Norwegian Beamline at the ESRF in Grenoble. To ensure that the sample was fully rehydrated, a previously established procedure was followed. The calcined sample was kept overnight in moist air at a temperature of 10 °C. The powder was then sealed into a 1-mm capillary and kept at 10 °C in a cryostat for the data collection. Further details are given in Table 1.

Indexing of the powder pattern of the rehydrated phases was performed using the indexing programs TREOR[32] and ITO,[33] and the structure analysis was performed using the X-ray Rietveld System program package XRS-82.[34]

Results and Discussion

The X-ray powder diffraction pattern of the as-synthesized triclinic $AlPO_4$-34 sample is similar to those reported previously. Its sharp lines are indicative of a highly pure and crystalline material (Figure 1a). After calcination, the powder pattern could be indexed on a rhombohedral unit cell that is consistent with the **CHA** topology and that is also observed for MeAPO-34 and SAPO-34 prepared in the absence of fluoride ions.

The X-ray powder diffraction pattern of rehydrated $AlPO_4$-34 is quite different from that of the calcined rhombohedral material (Figure 1). There are many more peaks, indicating a lower symmetry, and these are very sharp, indicating an excellent crystallinity, which is rather unusual for hydrated aluminophosphate molecular sieves. A detailed comparison of several rehydrated samples of $AlPO_4$-34 revealed that most of them were actually mixtures of two phases that could also be

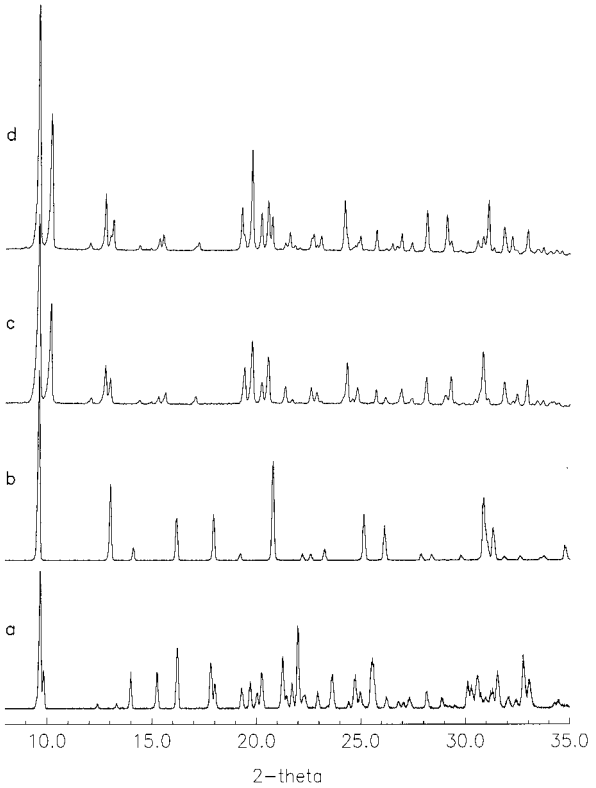

Figure 1. X-ray powder diffraction patterns of $AlPO_4$-34: (a) as-synthesized, (b) calcined, (c) rehydrated phase A, and (d) rehydrated phase B.

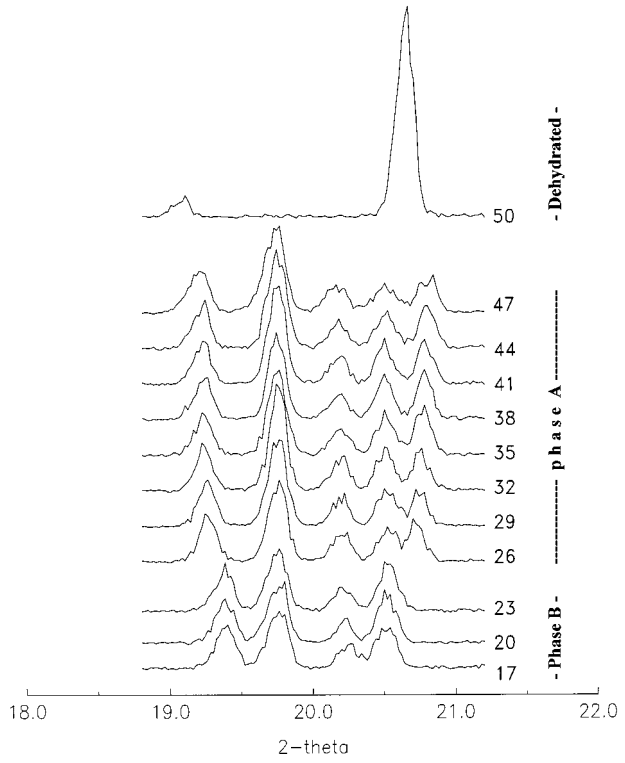

Figure 2. Sections of the X-ray powder diffraction patterns collected during an in situ experiment showing the phase transitions from rehydrated phase B to rehydrated phase A to completely dehydrated $AlPO_4$-34. The corresponding temperatures (in °C) are indicated for each pattern.

obtained pure (phases A and B in Figure 1). Initially, the existence of the two phases was thought to be time-dependent (one phase was assumed to be incompletely hydrated) and the hydration process to be slow. However, by following the rehydration process using powder diffraction techniques (Figure 2), it became clear that the phase transitions are in fact very fast and (at approximately constant humidity) only temperature-dependent.

Figure 2 shows characteristic parts of the diffraction patterns during the dehydration of rehydrated $AlPO_4$-34 collected in situ on heating at ambient humidity from 17 °C to 50 °C in steps of 3 °C. The low-temperature phase B changes to phase A between 23 and 26 °C, and phase A transforms to the rhombohedral water-free phase between 47 and 50 °C. Several cycles of cooling and heating, immediately following an in situ calcination, revealed that all phase transitions are fast and completely reversible. All phases remain highly crystalline even after several rehydration−dehydration cycles.

A comparison with TGA results revealed that the two phase transitions occur at the onset of abrupt weight losses (the beginning of peaks on the DTG curve in Figure 3). The peak temperatures on the DTG curve are at somewhat higher temperatures than those found by X-ray diffraction. One reason for this probably lies in the fact that the sample packing in the crucible for the TGA is denser than that of the very thin layer mounted on the Pt heating filament of the HTK chamber. The transition from phase B to phase A is accompanied by the desorption of one water molecule per unit cell, whereas phase A transforms to completely dehydrated rhombohedral $AlPO_4$-34 upon losing approximately 11 water molecules per unit cell. In the TGA experiment, the sample was completely dehydrated at 75 °C.

Once they had been identified, phases A and B could be indexed readily with the programs TREOR and ITO. The two

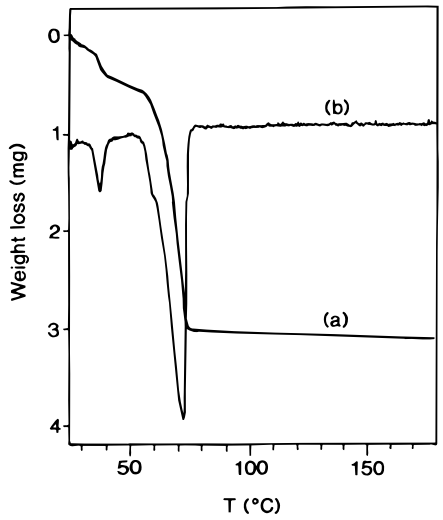

Figure 3. TG (a) and DTG (b) curves for rehydrated $AlPO_4$-34 (phase B).

programs gave identical results with high figures-of-merit. Both phases have triclinic unit cells (phase A: $a = 9.010$ Å, $b = 9.279$ Å, $c = 9.584$ Å, $\alpha = 95.23°$, $\beta = 104.93°$, $\gamma = 95.33°$, phase B: $a = 9.026$ Å, $b = 9.338$ Å, $c = 9.508$ Å, $\alpha = 95.08°$, $\beta = 104.08°$, $\gamma = 96.59°$) that are closely related to that of the rhombohedral calcined phase ($a \approx 9.4$ Å, $\alpha \approx 94°$).

The similarity of the unit cells and the reversibility of all phase transitions suggested that all framework bonds remain intact during rehydration and that the adsorption of water just breaks the 3-fold axis characteristic of the rhombohedral phase. The unit cell of the dehydrated rhombohedral phase contains six Al, six P, and 24 O atoms. All atoms occupy general positions in the space group *R*3 (multiplicity 6), so the six Al

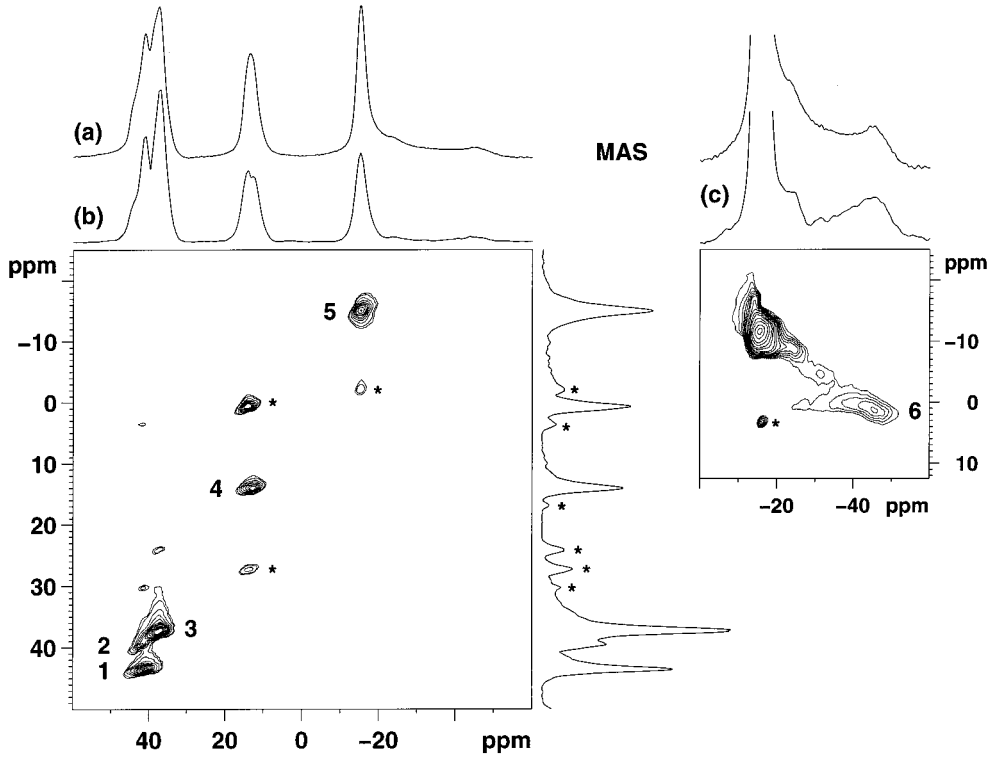

Figure 4. ^{27}Al MAS (a) and ^{27}Al 2D-5Q MAS (b) NMR spectra of rehydrated $AlPO_4$-34. For the region characteristic of 6-coordinate aluminum species (c), the intensity was enlarged by a factor of 5. Asterisks denote spinning sidebands.

and the six P atoms are symmetrically equivalent, and there are only 4 O atoms in the asymmetric unit. On the basis of the similar shapes and volumes of the unit cells of the two rehydrated phases, it was expected that they would contain the same number of framework atoms (6 Al, 6 P, and 24 O) and additional water molecules in the channels.

A series of diffraction experiments showed that phase A is rather unstable and that the A ↔ B phase transition depends strongly on the conditions for adsorbing/desorbing water. Furthermore, it was found that even in a closed capillary held at controlled constant temperature, some peaks in the diffraction pattern of phase A moved during the data collection, so a Rietveld refinement of this structure was not possible. This lack of stability of phase A and the conditions influencing the A ↔ B transition made it impossible to be sure that the NMR spectra collected were of the pure phase A. It was never clear whether the phase in the MAS NMR sample holder was really pure or in fact a mixture.

However, standard ^{27}Al and ^{31}P MAS and ^{27}Al 2D-5Q MAS NMR experiments performed at temperatures between −20 °C and 50 °C did not show any significant changes in the spectra, anyway. This suggests that the coordination spheres and environments of the framework atoms are the same in both phases (Figure 4). Both ^{27}Al and ^{31}P MAS NMR spectra (Figures 4 and 5) are very different from those of the dehydrated rhombohedral phase, which display a single signal at ca. 33 ppm and at −29 ppm for the ^{27}Al and the ^{31}P nuclei, respectively. This is consistent with the presence of only one crystallographic site in that structure.

Phase B is much more stable than phase A, and a synchrotron data collection at controlled temperature yielded a high quality pattern that could be used for structure refinement. All further results thus apply to phase B, which can be regarded as completely rehydrated.

An important question was whether the structure is centrosymmetric or not, and an essential indication of the correct answer came from the NMR experiments. The solid state ^{31}P MAS NMR spectrum of the fully rehydrated material is composed of 5 distinct Gaussian lines between −22 and −28 ppm, each one with a fwhm of approximately 250 Hz and with the relative intensities 1:1:1:2:1 (Figure 5 and Table 2). This suggests the presence of at least five (probably six) different environments for the P atoms in the unit cell and therefore points toward a noncentrosymmetric structure (space group *P*1). This result was supported by ^{27}Al MAS NMR. The ^{27}Al MAS NMR spectrum of the rehydrated compound (Figure 4a) shows signals around 40, 16, and −12 ppm with relative intensities of ca. 3:1:2, which also suggests the existence of 6 nonequivalent

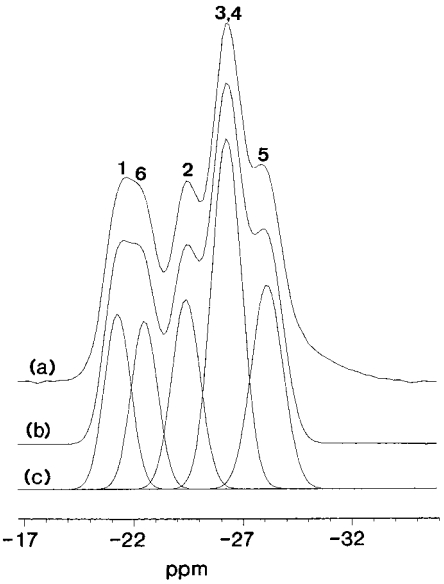

Figure 5. ^{31}P MAS NMR spectrum of rehydrated $AlPO_4$-34: experimental (a), simulated (b), and deconvoluted with Gaussian lines (c). Peak labeling was made according to the assignment in Table 2.

TABLE 2: Observed and Calculated ^{31}P NMR Chemical Shifts and Line Widths for Rehydrated $AlPO_4$-34

site	chemical shift (ppm) observed	chemical shift (ppm) calculated[a]	difference (ppm)	line width (Hz)
P1	−21	−28.1	7.1	248
P2	−24.3	−29.2	4.9	249
P3	−26.2	−29.3	3.1	272
P4	−26.2	−29.4	3.2	272
P5	−28.2	−29.8	1.6	285
P6	−22.5	−27.0	4.5	250

[a] Calculated from ref 39.

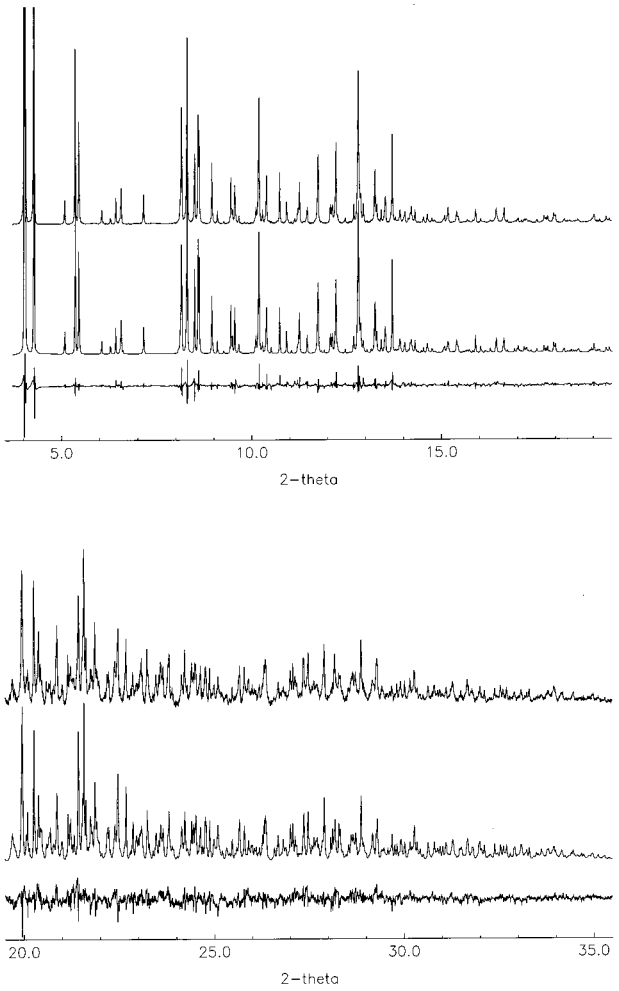

Figure 6. Final Rietveld plot of rehydrated $AlPO_4$-34 (phase B). Observed, calculated, and difference profiles are shown from top to bottom. To show more detail, the first peak has been cut at about 30% of its intensity, and for the same reason, the second part has been scaled up by a factor of 10.

aluminum species. Furthermore, the NMR results provided information on the probable cause of the deformation of the structure. From the chemical shifts in the ^{27}Al spectrum, it was possible to derive the coordination numbers of the Al species: 2 Al are 6-coordinate ($-12 < \delta < -45$ ppm), 1 Al is 5-coordinate ($\delta \approx 16$ ppm), and 3 Al are 4-coordinate ($\delta \approx 40$ ppm).

On the basis of the unit cell, the known structure of the rhombohedral phase, and the indication of the space group and coordination of Al sites, it was possible to build an initial model for Rietveld refinement. Atomic coordinates of all of the atoms in the rhombohedral structure were used, and then a geometry optimization using DLS-76[35] was performed in the triclinic unit cell assuming all Al and P atoms to be tetrahedrally coordinated.

TABLE 3: Positional and Isotropic Displacement Parameters for Rehydrated $AlPO_4$-34 (Phase B)[a]

atom	*x*	*y*	*z*	*U*(Å^2)	PP[b]
P(1)	0.3591	0.8857	0.1227	0.032(1)[c]	
P(2)	0.104(2)	0.332(2)	0.877(2)	0.032(1)[c]	
P(3)	0.949(2)	0.102(2)	0.313(2)	0.032(1)[c]	
P(4)	0.650(2)	0.124(1)	0.874(1)	0.032(1)[c]	
P(5)	0.925(2)	0.654(2)	0.134(2)	0.032(1)[c]	
P(6)	0.048(2)	0.878(2)	0.653(2)	0.032(1)[c]	
Al(1)	0.302(2)	0.089(2)	0.880(2)	0.039(1)[d]	
Al(2)	0.905(2)	0.329(2)	0.099(2)	0.039(1)[d]	
Al(3)	0.176(3)	0.866(2)	0.377(2)	0.039(1)[d]	
Al(4)	0.686(2)	0.879(2)	0.078(2)	0.039(1)[d]	
Al(5)	0.108(2)	0.669(2)	0.893(2)	0.039(1)[d]	
Al(6)	0.833(2)	0.129(2)	0.618(2)	0.039(1)[d]	
O(1)	0.203(3)	0.979(3)	0.718(3)	0.037(1)[e]	
O(2)	0.260(3)	0.759(2)	0.019(3)	0.037(1)[e]	
O(3)	−0.009(3)	0.244(3)	0.750(3)	0.037(1)[e]	
O(4)	0.726(3)	0.257(3)	0.980(3)	0.037(1)[e]	
O(5)	0.803(3)	1.005(3)	0.224(3)	0.037(1)[e]	
O(6)	0.052(3)	0.716(3)	0.261(3)	0.037(1)[e]	
O(7)	0.354(3)	0.020(2)	0.044(3)	0.037(1)[e]	
O(8)	0.249(3)	0.264(3)	0.889(3)	0.037(1)[e]	
O(9)	0.063(3)	0.338(3)	0.021(3)	0.037(1)[e]	
O(10)	0.975(3)	0.253(3)	0.262(3)	0.037(1)[e]	
O(11)	0.085(3)	0.019(3)	0.301(3)	0.037(1)[e]	
O(12)	0.316(3)	0.907(3)	0.269(2)	0.037(1)[e]	
O(13)	0.711(3)	0.999(3)	0.954(3)	0.037(1)[e]	
O(14)	0.774(3)	0.720(3)	0.113(3)	0.037(1)[e]	
O(15)	0.977(3)	0.651(3)	0.997(3)	0.037(1)[e]	
O(16)	0.039(4)	0.743(3)	0.733(3)	0.037(1)[e]	
O(17)	0.914(3)	0.960(3)	0.668(3)	0.037(1)[e]	
O(18)	0.701(3)	0.111(3)	0.737(2)	0.037(1)[e]	
O(19)	0.477(2)	0.108(3)	0.840(3)	0.037(1)[e]	
O(20)	0.528(2)	0.863(3)	0.157(3)	0.037(1)[e]	
O(21)	0.878(3)	0.498(2)	0.158(3)	0.037(1)[e]	
O(22)	0.144(4)	0.492(2)	0.851(3)	0.037(1)[e]	
O(23)	0.040(3)	0.837(3)	0.495(3)	0.037(1)[e]	
O(24)	0.943(3)	0.139(3)	0.474(3)	0.037(1)[e]	
O(31)	0.271(5)	0.712(4)	0.475(4)	0.135(4)[f]	1.250[h]
O(32)	0.341(4)	0.988(4)	0.534(4)	0.135(4)[f]	1.250[h]
O(33)	0.659(4)	−0.011(4)	0.479(4)	0.135(4)[f]	1.250[h]
O(34)	0.733(5)	0.305(4)	0.543(4)	0.135(4)[f]	1.250[h]
O(35)	0.068(3)	0.014(4)	−0.031(4)	0.135(4)[f]	1.250[h]
O(36)	0.549(4)	0.755(3)	−0.098(3)	0.135(4)[f]	1.250[h]
O(41)	0.674(4)	0.705(4)	0.625(4)	0.162(6)[g]	1.250[h]
O(42)	0.102(3)	0.473(4)	0.502(4)	0.162(6)[g]	1.250[h]
O(43)	0.486(6)	0.487(4)	−0.005(6)	0.162(6)[g]	1.250[h]
O(44)	0.433(4)	0.553(4)	0.285(3)	0.162(6)[g]	1.250[h]
O(45)	0.463(4)	0.237(4)	0.310(4)	0.162(6)[g]	1.250[h]
O(46)	0.341(3)	0.322(4)	0.537(3)	0.162(6)[g]	1.250[h]

[a] Numbers in parentheses are the estimated standard deviations in the units of the least significant digit given. [b] Population parameter. [c−g] Displacement parameters with the same superscript were constrained to be equal. [h] Hydrogen atoms of the water molecules were not located. These population parameters were increased to approximate the total scattering power of H_2O.

Because Al and P are interchangeable in the rhombohedral structure (the interchange is equivalent to a redefinition of the origin) but not in the triclinic one, two starting models were needed, and the Rietveld refinement was started using both. After a few iterations of partial restrained refinement followed by the calculation of a difference Fourier map, it became clear which model was the correct one.

This initial model was still incorrect in two respects: (1) the water in the channels and/or bound to specific Al atoms was missing, and (2) all Al atoms were assumed to be tetrahedrally coordinated to framework oxygens. Both of these approximations were improved simultaneously using an iterative procedure. First, a highly restrained refinement using only the high-angle (*d*-spacing below 3.0 Å) part of the pattern was performed. This

TABLE 4: Bond Lengths and Angles for Rehydrated $AlPO_4$-34 (Phase B)

Bonds (Å)

P1	O2	1.52(2)	P3	O11	1.55(4)	P6	O23	1.50(3)	Al3	O6	1.79(3)	Al5	O16	1.74(3)
P1	O12	1.53(2)	P4	O4	1.51(2)	P6	O17	1.53(4)	Al3	O12	1.85(4)	Al5	O22	1.75(3)
P1	O20	1.52(2)	P4	O18	1.49(3)	Al1	O8	1.76(3)	Al3	O23	1.87(4)	Al5	O15	1.72(4)
P1	O7	1.52(2)	P4	O19	1.50(2)	Al1	O19	1.71(3)	Al3	O31	1.94(5)	Al5	O2	1.67(3)
P2	O3	1.48(3)	P4	O13	1.53(3)	Al1	O1	1.75(3)	Al3	O32	1.99(4)	Al6	O18	1.83(4)
P2	O8	1.50(4)	P5	O14	1.53(4)	Al1	O7	1.72(3)	Al3	O11	1.85(4)	Al6	O24	1.88(4)
P2	O22	1.56(3)	P5	O21	1.53(3)	Al1	O35	2.51(4)	Al4	O5	1.77(3)	Al6	O33	2.03(4)
P2	O9	1.51(4)	P5	O15	1.48(3)	Al2	O10	1.77(3)	Al4	O14	1.79(4)	Al6	O34	2.06(5)
P3	O10	1.54(3)	P5	O6	1.47(3)	Al2	O21	1.69(3)	Al4	O20	1.77(3)	Al6	O17	1.87(4)
P3	O24	1.56(3)	P6	O1	1.55(3)	Al2	O4	1.75(3)	Al4	O36	2.00(3)	Al6	O3	1.81(3)
P3	O5	1.52(3)	P6	O16	1.53(3)	Al2	O9	1.76(4)	Al4	O13	1.73(3)			

Angles (°)

O2	P1	O12	113.2(14)	O1	P6	O23	107(2)	O23	Al3	O32	94.7(17)	O33	Al6	O17	84.0(16)
O2	P1	O20	110.1(14)	O1	P6	O17	109.8(18)	O23	Al3	O11	92.6(18)	O33	Al6	O3	176(2)
O2	P1	O7	108.5(12)	O16	P6	O23	111(2)	O31	Al3	O32	81.1(17)	O34	Al6	O17	174.4(17)
O12	P1	O20	107.1(14)	O16	P6	O17	108(2)	O31	Al3	O11	175(2)	O34	Al6	O3	92.6(16)
O12	P1	O7	113.1(15)	O23	P6	O17	111(2)	O32	Al3	O11	95.7(16)	O17	Al6	O3	92.4(15)
O20	P1	O7	104.3(14)	O8	Al1	O19	105.5(17)	O5	Al4	O14	100.4(15)	P6	O1	Al1	139(2)
O3	P2	O8	104.4(19)	O8	Al1	O1	113.2(16)	O5	Al4	O20	93.7(16)	P1	O2	Al5	157.8(19)
O3	P2	O22	113.2(19)	O8	Al1	O7	116.1(16)	O5	Al4	O36	174.3(17)	P2	O3	Al6	170(2)
O3	P2	O9	117(2)	O8	Al1	O35	86.1(16)	O5	Al4	O13	90.8(15)	P4	O4	Al2	140(2)
O8	P2	O22	106(2)	O19	Al1	O1	95.6(16)	O14	Al4	O20	104.7(17)	Al4	O5	P3	157(2)
O8	P2	O9	109(2)	O19	Al1	O7	99.0(16)	O14	Al4	O36	84.9(14)	Al3	O6	P5	152(2)
O22	P2	O9	106(2)	O19	Al1	O35	166.7(18)	O14	Al4	O13	129(2)	P1	O7	Al1	146.9(15)
O10	P3	O24	103.3(18)	O1	Al1	O7	122.0(16)	O20	Al4	O36	87.1(15)	P2	O8	Al1	137(2)
O10	P3	O5	114.9(18)	O1	Al1	O35	85.4(14)	O20	Al4	O13	124.4(17)	Al2	O9	P2	142.2(18)
O10	P3	O11	109(2)	O7	Al1	O35	69.6(14)	O36	Al4	O13	84.1(14)	P3	O10	Al2	134.9(17)
O24	P3	O5	111(2)	O10	Al2	O21	104.1(17)	O16	Al5	O22	109.7(17)	P3	O11	Al3	139(2)
O24	P3	O11	112(2)	O10	Al2	O4	121.1(17)	O16	Al5	O15	113.4(18)	P1	O12	Al3	148.6(16)
O5	P3	O11	105.8(18)	O10	Al2	O9	102.2(17)	O16	Al5	O2	119.1(17)	Al4	O13	P4	146(2)
O4	P4	O18	114.9(17)	O21	Al2	O4	103.1(16)	O22	Al5	O15	105.0(19)	P5	O14	Al4	145(2)
O4	P4	O19	112.3(17)	O21	Al2	O9	110.0(19)	O22	Al5	O2	108.8(17)	P5	O15	Al5	156.1(18)
O4	P4	O13	103.6(14)	O4	Al2	O9	115.5(16)	O15	Al5	O2	99.7(16)	P6	O16	Al5	146.0(18)
O18	P4	O19	110.1(16)	O6	Al3	O12	100.5(16)	O18	Al6	O24	171.8(15)	Al6	O17	P6	140(2)
O18	P4	O13	104.2(18)	O6	Al3	O23	83.3(16)	O18	Al6	O33	81.4(16)	P4	O18	Al6	157.8(17)
O19	P4	O13	111.2(17)	O6	Al3	O31	83.0(16)	O18	Al6	O34	89.2(19)	P4	O19	Al1	155(2)
O14	P5	O21	103(2)	O6	Al3	O32	164(2)	O18	Al6	O17	92.7(18)	P1	O20	Al4	139.7(19)
O14	P5	O15	110(2)	O6	Al3	O11	100.1(15)	O18	Al6	O3	97.0(15)	P5	O21	Al2	139(3)
O14	P5	O6	118(2)	O12	Al3	O23	176.0(17)	O24	Al6	O33	90.9(16)	P2	O22	Al5	143(3)
O21	P5	O15	108(2)	O12	Al3	O31	98(2)	O24	Al6	O34	88.1(19)	P6	O23	Al3	134.7(18)
O21	P5	O6	106.1(18)	O12	Al3	O32	82.0(16)	O24	Al6	O17	89.3(18)	P3	O24	Al6	149.7(19)
O15	P5	O6	111(2)	O12	Al3	O11	85.5(17)	O24	Al6	O3	90.9(15)				
O1	P6	O16	110.8(18)	O23	Al3	O31	84(2)	O33	Al6	O34	91.1(16)				

Hydrogen Bonds (Å)

O31	O42	2.62(5)	O33	O34	2.92(5)	O36	O43	2.77(5)	O43	O44	2.93(7)
O31	O44	2.99(6)	O34	O45	2.83(5)	O42	O46	2.68(5)	O45	O46	2.75(5)

produced an approximately correct scaling of the calculated pattern to the observed one,[36] while the strong restraints kept the bond distances and angles within reason (though they were forcing some Al atoms to adopt incorrect coordination geometries). Then, a difference Fourier map was calculated using the whole pattern. Analysis of the difference map was focused on finding the peaks at about 2.0 Å from Al atoms and considering the peaks very close (within 1 Å) to Al or P that could be "true" positions of Al and P atoms, which had been displaced as a result of the incorrect restraints. This analysis resulted in the location of possible positions for coordinated water and the correction of the restraints for the Al atom to which the water was bound. Only one water molecule was added per iteration, and then the process was repeated. After the coordinated water molecules had been located, rather well-defined positions for the water molecules in the chabazite cage H-bonded either to framework oxygens and/or to other water molecules also appeared. During this process, the weight of the restraints and the "high-angle" limit were gradually decreased, so that the final refinement was performed with the whole pattern and a restraint weight of 1.0.

The population parameters of the water molecules not bound to Al atoms could have been lower than 1.0, but several refinement trials were indicative of full occupancy. Therefore, the occupancy factors for the water molecule oxygens were fixed at 1.25 (to account for the scattering power of the two unlocated hydrogen atoms) in the final cycles of refinement. The atomic displacement parameters were refined isotropically and those for the same kind of atom were constrained to be equal (coordinated and "free" water molecules were considered to be different).

After 12 water molecules per unit cell had been located, there were no significant misfits in the integrated intensities of the observed and calculated patterns. The refinement of the unit cell, all positional (except those of P1 which were origin fixing coordinates) and grouped atomic displacement parameters converged to a sensible structure, but the profile R values remained rather high. Furthermore, the difference profile showed some obvious profile misfits as a result of anisotropic line broadening and a very irregular behavior of the peak asymmetry. Because of the very high resolution, there were many isolated peaks at low angles that could be fitted separately to establish

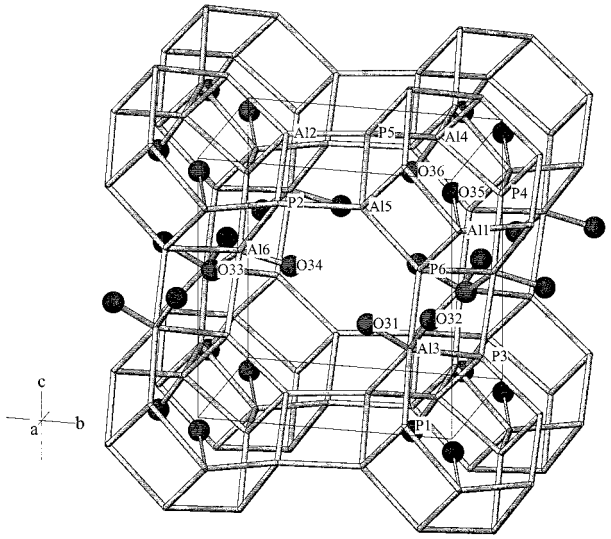

Figure 7. The framework structure of rehydrated $AlPO_4$-34 (phase B) showing just the Al and P atoms (at the nodes) and the coordinated water molecules (balls). Bridging oxygen atoms and "free" water molecules have been omitted for clarity. The atoms of one asymmetric unit are labeled.

individual profile parameters. A lot of effort was put into finding a rule to describe the irregular behavior, but none could be found. The asymmetry parameters, which in some cases showed clearly "negative" values (those peaks had an asymmetric "tail" on the high-angle side), in particular, finally led us to the conclusion that these effects are probably due to diffuse scattering originating from a rather complicated disorder, which we could not model.

To improve the fit and to include the full intensity from peaks with long tails, the profile parameters of the isolated peaks were refined independently and then kept constant in the final cycles of refinement when the unit cell and all atomic parameters were refined to convergence. The final Rietveld plot for the refinement of the fully hydrated phase B is given in Figure 6. Atomic coordinates and selected bond lengths and angles are presented in Tables 3 and 4, respectively.

The rehydrated phase B contains twelve molecules of water per unit cell. Five of them are coordinated to Al atoms with bond lengths of about 2.0 Å to give two 6-coordinate and one 5-coordinate aluminum species. A sixth water molecule is located within a double 6-ring (D6R) of the framework. It is positioned off the center of the D6R so that it avoids close contact with all P and O atoms, but it may be regarded as "quasi" coordinated to one Al atom at a distance of about 2.5 Å. The other six water molecules fill the chabazite cage at quite well-defined positions.

This structural study clearly reveals how the coordinated water molecules affect the symmetry. The structure can be viewed in terms of 4-rings, which connect double 6-rings along the three unit cell axes (Figure 7). Each 4-ring contains two Al atoms. In the 4-rings along the *c* direction, two pairs of water molecules coordinate to Al3 and Al6, making them 6-coordinate. The 4-rings along the *a* direction contain Al1 and Al4, where Al4 is 5-coordinate and Al1 can be regarded as 4+1-coordinate (the distance to the "coordinating" water molecule is rather high, and this Al is seen as 4-coordinate by NMR). In the 4-rings along the *b* direction, Al2 and Al5 remain 4-coordinate as in the calcined material. The deformation of the framework caused by the changes in the coordination spheres of the other Al atoms prevent water molecules from coming close enough to coordinate to these two Al atoms.

The environment around each P and Al atom of the framework was also investigated by solid-state NMR and the results compared with those from the diffraction experiment. As previously mentioned, both ^{31}P and ^{27}Al MAS NMR spectra confirm that the structure of rehydrated $AlPO_4$-34 contains six nonequivalent framework Al and P sites. Moreover, ^{27}Al 2D-5Q MAS NMR indicates that three of the framework Al species are 4-coordinate, one is 5-coordinate and two are 6-coordinate (Figures 4b and 4c). These results reflect the rehydration process of $AlPO_4$-34. Of the three 4-coordinate aluminum sites in the rehydrated form, two have a very similar environment and symmetry (Al2 and Al5 in Figure 7). It is therefore logical to assign them to the overlapping resonances at 40 ppm in the MAS spectrum, which can be resolved with the superior

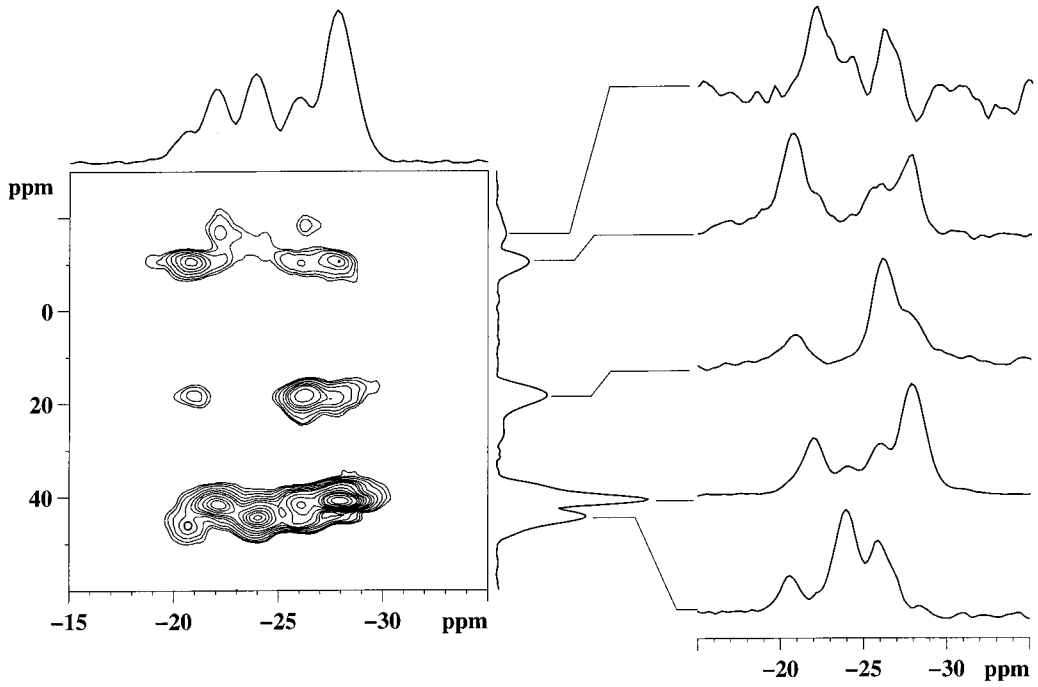

Figure 8. $^{27}Al-^{31}P$ CP/MAS NMR correlation spectrum of rehydrated $AlPO_4$-34. ^{31}P peak labeling was made according to Table 2.

TABLE 5: Observed and Calculated Quadrupolar Coupling Constants for the Aluminum Sites of Rehydrated $AlPO_4$-34

NMR signal[a]	site	coupling constant (MHz)[b] observed	calculated[c]
1	Al1	3.9	2.6
2	Al2, Al5	3.0	1.6
3	Al2, Al5	3.2	0.9
4	Al4	2.9	
5	Al3	2.7	
6	Al6	7.3	

[a] The signal numbers correspond to those in Figure 4. [b] Evaluated assuming $\eta = 0$, which involves a maximum error of ±15%. [c] Calculated from the data of ref 37 for tetrahedral sites only.

resolution of the 2D 5Q MAS spectrum (sites 2 and 3 in Figure 4b). The third signal in the tetrahedral region of the spectrum, at 43.5 ppm, can be then assigned to Al1, which possesses a neighboring, noncoordinating water molecule (2.5 Å).

The presence of water appears to influence the NMR spectrum of aluminophosphates in several ways. For example, the ^{27}Al resonances corresponding to the Al species that do not change upon rehydration are shifted by 5 to 10 ppm to lower fields in the rehydrated material. Such a deshielding effect may be indicative of some hydrogen bonding between the water molecules and the oxygen in the coordination sphere of the aluminum. In addition, an effect on the quadrupolar coupling constants seems to appear. On the basis of both theoretical and experimental results, Engelhardt et al.[37] have suggested a linear correlation between the quadrupolar coupling interaction of 4-coordinate Al sites and the distortion of the local geometry from an ideal tetrahedron. This formula was successfully tested against a number of aluminosilicate materials as well as the aluminophosphate VPI-5. However, when we apply this method to the current structure, we obtain a discrepancy between the observed (through the 5Q-MAS) and calculated quadrupolar parameters (Table 5). It is possible that the electric field gradient (EFG) around the aluminum center is modulated by the presence of a dielectric medium and/or by the emergence of hydrogen bonds between the water and the framework oxygens.[38] Such a hypothesis needs to be further rationalized both by theoretical modeling and further experiments on a larger set of hydrated aluminophosphates. As far as the region of the spectrum corresponding to the 6-coordinate aluminum species is concerned (Figure 4c), signal 5 with the smallest C_Q value can be assigned to the more symmetrical octahedral site Al3 (Table 4). The remaining signal (signal 6) has a strong quadrupolar coupling constant (Table 5) and thus corresponds to Al6, for which the octahedron is distorted by the presence of two long Al−O distances (Table 4).

Assignment of ^{31}P NMR lines is more difficult, because all P atoms of the framework are 4-coordinate and the chemical shift variation is quite small. Müller et al.[39] have proposed an empirical relationship between the mean P−O−Al bond angle in the structure of aluminophosphates (Φ) and the corresponding chemical shift (δ):

$$\delta(\text{ppm}) = 47 - 0.51\Phi$$

This correlation has often been used as a semiquantitative tool to assign ^{31}P NMR signals in various $AlPO_4$ materials. The results for hydrated $AlPO_4$-34 are listed in Table 2. All calculated chemical shifts lie within a much narrower range than do the experimentally observed ones. The only noticeable exceptions are P1 and P6. Again, this is probably due to the presence of the extra molecule of water in the structure (O35 in Figure 7), not far from the positions of those two atoms.

TABLE 6: Framework Connectivities Obtained from the Structure Plotted in Figure 7

	P1	P2	P3	P4	P5	P6
Al1	×	×		×		×
Al2		×	×	×	×	
Al3	×		×		×	×
Al4	×		×	×	×	
Al5	×	×			×	×
Al6		×	×	×		×

To progress in the assignment procedure, a heteronuclear correlation experiment was performed to elucidate the spatial proximity (Figure 8). In fact, the presence of a nonvanishing dipolar coupling between Al and P is indicative of distances of less than 4 Å. In this case, it is possible to perform a $^{27}Al-^{31}P$ cross-polarization experiment in which the presence of a peak in a 2D diagram at the frequency of Al and P reflects the structure connectivities (Table 6) and reveals the spatial proximity.

It is then possible to use the Al assignment to interpret the ^{31}P spectrum (Figure 5). For example, Al1, with its characteristic chemical shift of 43.5 ppm, correlates, according to the structure, to P1, P2, P4, and P6 (Table 6, Figure 8). By inspection of the corresponding trace, the signal at −28.2 ppm can be assigned to P5. The 5-coordinate Al4 is neighboring P1, P3, P4, and P5. The corresponding trace shows that P1 resonates at −21 and P3 and P4 at −26.2. At this point, it is possible to resolve the assignment of the octahedral Al3 (which connects with P1, P3, P5, and P6) to the signal at −10 ppm, because the Al6, which resonates at −17 ppm, does not correlate to P1. The last ambiguity in the phosphorus MAS spectrum (P2 and P6) is lifted by noting that Al3 correlates to P6 but not to P2, which are then assigned to the resonances at −22.5 and −24.3 ppm, respectively.

It is interesting to note the deviation between the observed ^{31}P chemical shift and the ones calculated according to ref 39 (Table 2). As was also observed for the aluminum signals, all resonances are shifted upfield with respect to the calculation. The largest deviation from the calculated value is relative to P1, which shares a bridging oxygen with Al1. This observation reinforces the hypothesis of hydrogen bonding of a water molecule to this oxygen. P5, on the other hand, seems to be least affected by the presence of water.

Conclusions

The triclinic structure of the microporous aluminophosphate obtained by calcination and subsequent rehydration of as-synthesized $AlPO_4$-34 was studied by X-ray diffraction and solid-state NMR. Following the rehydration of the calcined $AlPO_4$-34 (rhombohedral) in situ revealed that two different hydrated phases were formed, both with triclinic symmetry. The transition between these two phases was found to occur reversibly at ca. 25 °C and to be accompanied by the adsorption/desorption of one water molecule per unit cell. The structure of the fully hydrated low-temperature phase has been elucidated using X-ray powder diffraction techniques. The unit cell contains six nonequivalent P and Al atoms. Upon rehydration, aluminum atoms in the 4-rings along the *c*-axis become 6-coordinate, whereas those in 4-rings along the *b* direction remain 4-coordinate. Water also affects the aluminum atoms along the third direction: one of them becomes 5-coordinate, whereas the other remains 4-coordinate, with a water molecule ca. 2.5 Å away. Six additional water molecules occupy the empty space within the channels. Atom coordination numbers and framework connectivities derived from the structure analysis of the rehy-

drated phase were used, in combination with $^{27}Al-^{31}P$ CP/MAS correlation spectroscopy, to assign the ^{31}P NMR spectra completely and the ^{27}Al NMR spectra partially.

Acknowledgment. We would like to thank Drs. T. Wessels, J. de Oñate, and K. Knudsen and P. Pattison and Mr. H. Emmerich for their assistance with the synchrotron data collection. The Swiss−Norwegian Beamline is acknowledged for providing the beamtime. The Ministry of Science and Technology of the Republic of Slovenia and the Swiss National Science Foundation are also acknowledged.

References and Notes

(1) Wilson, S. T.; Lock, B. M.; Messina, C. A.; Cannan, T. R.; Flanigen, E. M. *J. Am. Chem. Soc*. **1982**, *104*, 1146.
(2) McCusker, L. B.; Baerlocher, Ch.; Jahn, E.; Büllow, M. *Zeolites* **1991**, *11*, 308.
(3) Pluth, J. J.; Smith, J. V. *Acta Crystallogr*. **1986**, *C42*, 283.
(4) Simmen, A.; McCusker, L. B.; Baerlocher, Ch.; Meier, W. M. *Zeolites* **1991**, *11*, 654.
(5) Flanigen, E. M.; Lock, B. M.; Patton, R. L.; Wilson, S. T. *Pure Appl. Chem*. **1986**, *58*(10), 1351.
(6) Wilson, S. T.; Flanigen, E. M. In *Zeolite Synthesis*; Occelli, M. L., Robson, H. E., Eds.; ACS Symposium Series 398; American Chemical Society: Washington, DC, 1989; p 329.
(7) Meussinger, J.; Vinek, H.; Lercher, J. A. *J. Mol. Catal*. **1994**, *87*, 263.
(8) Kraushaar-Czarnetzi, B.; Hoogervorst, W. G. M.; Stork, W. H. J. *Stud. Surf. Sci. Catal*. **1994**, *84*, 1869.
(9) Schott-Darie, C.; Kessler, H.; Benazzi, E. In *Proceedings of the International Symposium on Zeolite Microporous Crystals*, Nagoya, Japan, 1993; Hattori, T., Yashima, T., Eds.; Elsevier: Amsterdam, 1994; p 3.
(10) Kessler, H. In *Synthesis, Characterization and Novel Applications of Molecular Sieves Materials*; Bedard, R. L. et al., Eds.; Materials Research Society: Pittsburgh, 1991; Vol. 233, p 47.
(11) Simmen, A. PhD Thesis, University of Zürich, ETH N° 9710, Switzerland, 1992.
(12) Harding, M. H.; Kariuki, B. M. *Acta Crystallogr*. **1994**, *C50*, 852.
(13) Lesh, D. A.; Patton, R. L.; Woodward, N. A. Eur. Pat. Appl. 293939, 1998.
(14) Jahn, E.; Daniels, P.; Gies, H. *5th German Zeolite Workshop*, Leipzig, March 14−16, 1993.
(15) Hattmann, M.; Prakash, A. M.; Kevan, L. *J. Chem. Soc., Faraday Trans*. **1998**, *94*(5), 723.
(16) Caldarelli, S.; Meden, A.; Tuel, A. *J. Phys. Chem. B* **1999**, *103*, 5477.
(17) He, H.; Klinowski, J. *J. Phys. Chem*. **1993**, *97*, 10385.
(18) Peeters, M. P. J.; Van de Ven, L. J. M.; De Haan, J. W.; Van Hooff, J. H. C. *J. Phys. Chem*. **1993**, *97*, 8254.
(19) Peeters, M. P. J.; De Haan, J. W.; Van de Ven, L. J. M.; Van Hooff, J. H. C. *J. Phys. Chem*. **1993**, *97*, 5363.
(20) Khouzami, R.; Coudurier, G.; Lefebvre, F.; Vedrine, J. C.; Mentzen, B. F. *Zeolites* **1990**, *10*, 183.
(21) Mentzen, B. F.; Khouzami, R.; Vedrine, J. C. *C. R. Acad. Sci*. (Paris) **1987**, *304*, 11.
(22) Wu, G.; Rovnyak, D.; Griffin, R. G. *J. Am. Chem. Soc*. **1996**, *118*, 9326.
(23) Caldarelli, S.; Ziarelli, F. To be submitted for publication.
(24) Marion, D.; Würthrich, K. *Biochem. Biophys. Res. Commun*. **1983**, *113*, 967.
(25) Drobny, G.; Pines, A.; Sinton, S.; Weitekamp, D.; Wemmer, D. *Symp. Faraday Div. Chem. Soc*. **1979**, *13*, 49.
(26) Medek, A.; Harwood: J. S.; Frydman, L. *J. Am. Chem. Soc*. **1995**, *117*, 12779.
(27) Pines, A.; Gibby, M. G.; Waugh, J. S. *J. Chem. Phys*. **1973**, *59*, 569.
(28) Hartmann, S. R.; Hahn, E. *Phys. Rev*. **1962**, *128*, 2042.
(29) Vega, A. *J. Magn. Reson*. **1992**, *96*, 50.
(30) Sun, W.; Stephen, J. T.; Potter, L. D.; Wu, Y. *J. Magn. Reson*. **1995**, *116*, 181.
(31) Peersen, O. B.; Wu, X. L.; Kustanovitch, J.; Smith, S. O. *J. Magn. Res., Ser. A* **1993**, *104*(A), 334.
(32) Werner, P. E.; Eriksson, L.; Westdahl, M. *J. Appl. Crystallogr*. **1985**, *18*, 367.
(33) Visser, J. W. *J. Appl. Crystallogr*. **1969**, *2*, 89.
(34) Baerlocher, Ch. *XRS-82.The X-ray Rietveld System*; ETH: Zürich, 1982.
(35) Baerlocher Ch.; Hepp, A.; Meier, W. M. *DLS-76, a program for the simulation of crystal structures by geometric refinement*. ETH: Zürich, 1976.
(36) McCusker, L. B.; Von Dreele, R. B.; Cox, D. E.; Louer, D.; Scardi, P. *J. Appl. Crystallogr*. **1999**, *32*, 36.
(37) Engelhardt, G.; Veeman, W. *J. Chem. Soc., Chem. Commun*. **1993**, 622.
(38) Walter, T. H.; Oldfield, E. *J. Phys. Chem*. **1989**, *93*, 6744.
(39) Müller, D.; Jahn, E.; Ladwig, G.; Haubenreisser, U. *Chem. Phys. Lett*. **1984**, *109*, 332.